Constructing the GGE in integrable models: A Hilbert space Monte Carlo approach

Vincenzo Alba[1] and Maurizio Fagotti[2]

[1]*International School for Advanced Studies (SISSA), Via Bonomea 265, 34136, Trieste, Italy, INFN, Sezione di Trieste*
[2]*Département de Physique, Ecole normale superieure, CNRS, 24 rue Lhomond, 75005 Paris, France*
(Dated: June 25, 2015)

I. INTRODUCTION

$$\rho^{GGE} = \frac{1}{Z} \exp\left(-\sum_j \lambda_j \mathcal{I}_j\right) \quad (1)$$

We provide a Monte Carlo method to simulate the GGE statistica ensemble.

Remarkably, this allows to extract the rapidity densities defining the ensemble representative state in the thermodynamic limit.

Finite-size effects are under control and for moderately large chain sizes the Monte Carlo results agree very well with the thermodynamic limit results, especially for small rapidities. Higher rapidities are more sensitive to finite size effects as they reflec short length scales.

The method allows to address local observables for which the expression in terms of the rapidity is known as well.

An alternative numerical method would be Quantum Monte Carlo. However, this would require the implementation of the higher conserved charges, other than the Hamiltonian. As the range of higher charges becomes large this is not easily doable in practice.

We provide the first numerical verification of the validity of the GTBA equations for the Heisenberg spin chain.

Interestingly, finite-size corrections are generically small, i.e., expontially decaying with the chain size.

Our Monte Carlo approach can be trivially extended to include other conserved charges, both local and non-local, and arbitrary functions of the rapidities. While the former is related to the GGE average of the particle number, the latter measures its fluctuations. Notice that due to the $SU(2)$ symmetry of the conserved charges one has that $\langle S_z \rangle = 0$ (panel (g)).

The finite-size corrections for local observables are more carefully investigated in Fig. **??**, focusing on $\mathcal{I}_3$ and $\mathcal{I}_4$.

II. THE MODEL AND THE METHOD

A. The Heisenberg spin chain

The isotropic spin-$\frac{1}{2}$ Heisenberg (XXX) chain is defined by the Hamiltonian

$$\mathcal{H} \equiv J \sum_{i=1}^{L} \left[\frac{1}{2}(S_i^+ S_{i+1}^- + S_i^- S_{i+1}^+) + S_i^z S_{i+1}^z\right], \quad (2)$$

where $S_i^{\pm} \equiv (\sigma_i^x \pm i\sigma_i^y)/2$ are spin operators acting on the site i of the chain, $S_i^z \equiv \sigma_i^z/2$, and $\sigma_i^{x,y,z}$ the Pauli matrices. We fix $J = 1$ and use periodic boundary conditions identifying sites $L + 1$ and 1. Both the total spin $S_T^2 \equiv (\sum_i \vec{S}_i)^2$ and the total magnetization $S_T^z \equiv \sum_i S_i^z = L/2 - M$, with M number of down spins, commute with (2). Thus, the eigenstates of (2) can be labelled by M. Following the Bethe ansatz literature here we refer to the down spins as particles.

Each eigenstate of (2) is univocally identified by a set of M complex parameters (so-called rapidities) $-\infty < \{x_\alpha < \infty\}$ with $\alpha = 1, \ldots, M$. These are solutions of a set of non linear algebraic equations, the Bethe equations

$$\arctan(x_\alpha) = \frac{\pi}{L}J_\alpha + \frac{1}{L}\sum_{\beta \neq \alpha}\arctan\left(\frac{x_\alpha - x_\beta}{2}\right). \quad (3)$$

Here $J_\alpha \in \frac{1}{2}\mathbb{Z}$ are the Bethe quantum numbers. Any choice of $-L/2 \leq J_\alpha \leq L/2$ identifies a *finite* solution of the Bethe equations and an eigenstate of the XXX chain.

It can be shown that finite rapidities correspond to eigenstates of the XXX chain with maximum magnetization, i.e. $S_z = S$ (highest weight states). The associated descendant states are obtained by considering the solutions of the Bethe equations with $M' < M$ and supplementing the "missing" $M - M'$ rapidities with infinite ones.

B. The string hypothesis

An important feature of the Bethe equations (3) is that in the thermodynamic limit $L \to \infty$ the rapidities x_α form "string" patterns along the imaginary direction in the complex plane (string hypothesis). Specifically, the rapidities forming a string of length $1 \leq n \leq M$ (so-called n-string) are parametrized as

$$x_\gamma^{(n,j)} = x_\gamma^{(n)} - i(n - 1 - 2j), \quad j = 0, 1, \ldots, n-1, \quad (4)$$

where $x_\gamma^{(n)}\mathbb{R}$ is the real part of the string (string center), j labels the different rapidities in the same n-string, and γ denotes strings of the same length but with different centers.

One should stress that for finite-size chains (4) is not correct and deviations from the string pattern appear. However, these deviations typically decay exponentially with system size.

Substituting the string hypothesis (4) the Bethe equations (3), one obtains the discrete Bethe-Takahashi equations for the string centers as

$$2L \arctan(x_\gamma^{(n)}/n) = 2\pi I_\gamma^{(n)} + \sum_{(m,\beta) \neq (n,\gamma)} \Theta_{m,n}(x_\gamma^{(n)} - x_\beta^{(m)}).$$
$$(5)$$

Here the scattering phases $\Theta_{m,n}$ are defined as

$$\Theta_{m,n}(x) \equiv \begin{cases} \vartheta\left(\frac{x}{|n-m|}\right) + \sum\limits_{r=1}^{(n+m-|n-m|-1)/2} 2\vartheta\left(\frac{x}{|n-m|+2r}\right) + \vartheta\left(\frac{x}{n+m}\right) & \text{if} \quad n \neq m \\ \sum\limits_{r=1}^{n-1} 2\vartheta\left(\frac{x}{2r}\right) + \vartheta\left(\frac{x}{2n}\right) & \text{if} \quad n = m \end{cases},$$

where $\vartheta(x) \equiv 2\arctan(x)$. Similar to the Bethe quantum numbers the Bethe-Takahashi quantum numbers $I_\gamma^{(n)}$ identify the solutions of the Bethe-Takahashi equations. It can be shown that $I_\gamma^{(n)}$ are integers (half integers) if $L - \alpha_n$ is odd (even). Moreover, $I_\gamma^{(n)}$ obey the constraint

$$|I_\gamma^{(n)}| \leq \frac{1}{2}\left(L - 1 - \sum_{m=1}^{M} t_{mn}\alpha_m\right), \tag{6}$$

where $t_{mn} \equiv 2\min(m,n) - \delta_{mn}$. Given a set of solutions of (5), and correspondingly an eigenstate of (2), we define its "string content" as $\mathcal{S} \equiv \{\mu_1, \mu_2, \ldots, \mu_M\}$, with μ_n the number of n-strings. Clearly, one has that $\sum_{n=1}^{M} \mu_n = M$. The energy and the total momentum associated to a given solution of the Bethe-Takahashi equations are given as

$$E(\{I_\gamma^{(n)}\}) = -L/4 + \sum_{n,\gamma} \frac{2n}{(x_\gamma^{(n)})^2 + n^2} \tag{7}$$

$$K(\{I_\gamma^{(n)}\}) = \sum_{n,\gamma} \frac{2\pi I_\gamma^{(n)}}{L} \tag{8}$$

C. The thermodynamic limit

In the thermodynamic limit, i.e., for $L \to \infty$ the Bethe eigenstates are described by the distributions of the string centers ρ_n. These are defined such that $L\rho_n(x)$ gives the number of n-strings in the interval $[x, x+dx]$. More formally $\rho_n^p(x)$ can be defined as

$$\rho_n^p(x) \equiv \frac{1}{L(x_{\gamma+1}^{(n)} - x_\gamma^{(n)})} \tag{9}$$

The Bethe-Takahashi equations (5) are replaced by the integral equations

$$\rho_n^p(x) + \rho_n^h(x) = a_n(x) + \sum_{m=1}^{\infty} a_{nm}\rho_m^p(x) \tag{10}$$

Moreover, sum over eigenstates can be replaced by

$$\sum_{\text{states}} \to \int \mathcal{D}\boldsymbol{\rho}^p e^{S_{YY}[\boldsymbol{\rho}^p]}, \tag{11}$$

where $\boldsymbol{\rho}^p \equiv \{\rho_n^p\}_{n=1}^{\infty}$, and $S_{YY}[\boldsymbol{\rho}]$ is the Yang-Yang entropy

$$S_{YY}[\boldsymbol{\rho}] \equiv N \sum_{n=1}^{\infty} \int_{-\infty}^{+\infty} \rho_n(x) \log\left(1 + \frac{\rho_n^h(x)}{\rho_n(x)}\right)$$
$$+ \rho_n^h \log\left(1 + \frac{\rho_n(x)}{\rho_n^h(x)}\right). \tag{12}$$

The Yang-Yang entropy counts the number of eigenstates that in the thermodynamic limit lead to the same $\boldsymbol{\rho}$.

D. Hilbert space structure

For the XXX chain with L sites the total number of eigenstates with fixed number of particles M is given as $C_M^L - C_{M-1}^L$, with $C_y^x \equiv x!/(y!(x-y)!)$ the binomial coefficient. Thus, the probability of an eigenstate of the XXX chain with M particles is given as $(C_M^L - C_{M-1}^L)/C_{L/2}^L$.

For fixed M the total number of eigenstates $D(\mathcal{S})$ corresponding to a string content $\mathcal{S} \equiv \{\mu_1, \mu, \ldots, \mu_M\}$ is given as

$$D(\mathcal{S}) = \prod_{i=1}^{M} C_{\mu_i}^{L - \sum_{j=1}^{M} t_{ij}\mu_j}. \tag{13}$$

E. The conserved charges

Besides the total magnetization and the momentum, the XXX chain has non-trivial *local* conservation laws, due to the integrability. These extra conserved charges $\mathcal{I}_j$ can be obtained as

$$\mathcal{I}_{j+1} \equiv \frac{i}{(j-1)!} \frac{d^j}{dx^j} \log(\Lambda)\Big|_{x=i}. \tag{14}$$

Here Λ is the eigenvalue of the quantum transfer matrix $T(x)$ of the XXX chain, with x the spectral parameter. Notice that $\Lambda(x)$ depends on the solutions of the Bethe equations (3) $\{x_\alpha\}$ and it is given as

$$\Lambda \equiv \left(\frac{x+i}{2}\right)^L \prod_\alpha \frac{x - x_\alpha - 2i}{x - x_\alpha}$$
$$+ \left(\frac{x-i}{2}\right)^L \prod_\alpha \frac{x - x_\alpha + 2i}{x - x_\alpha}. \tag{15}$$

Notice that the second term in (15) does not contribute to the charges (cf. (14)), as long as $j < L$. It is trivial to check that $\mathcal{I}_1 \equiv K$ is the total momentum, while $\mathcal{I}_2 \equiv \mathcal{H}$. Moreover, the range of the conserved charge $\mathcal{I}_j$ is j, meaning that $\mathcal{I}_j$ acts non-trivially only on a block of j adjacent spins.

III. THE HILBERT SPACE MONTE CARLO SAMPLING

Here we describe the Hilbert space Monte Carlo approach to simulate the GGE ensemble. The method allows to calculate correlation functions and to extract the rapidity densities $\rho_n(x)$ of the ensemble representative state.

The basic idea of the method is to sample the Hilbert space, i.e., the eigenstates, of the XXX chain using a Metropolis algorithm.

Here we focus on a chain of length L. Given an eigenstate of the XXX chain in the sector with M particles and identified by a Bethe-Takahashi quantum number configuration $\mathcal{C}$, the basic Monte Carlo update generates another configuration $\mathcal{C}'$, and consists of five steps:

1. Select a particle number sector $0 \leq M \leq L/2$ with probability

$$P_{M'} = \frac{C_{M'}^L - C_{M'-1}^L}{C_{L/2}^L}. \qquad (16)$$

2. For fixed M' select the string content $\mathcal{S} = \{\mu_1, \mu_2, \ldots, \mu_{M'}\}$ with probability

$$P_{\mathcal{S}} = \frac{D(\mathcal{S})}{C_{L/2}^L}, \qquad (17)$$

where $D(\mathcal{S})$ given in (13).

3. Generate randomly a Bethe-Takahashi quantum number configuration $\mathcal{C}'$ consistent with the string content $\mathcal{S}$ obtained in step 2.

4. Solve the Bethe-Takahashi equations (5) for using the quantum number configuration $\mathcal{C}'$ obtained in step 3. Obtain the value of the conserved charges $\mathcal{I}_j'$ with $j = 2, m$.

5. Accept the new configuration with the Metropolis probability $T(\mathcal{C} \to)\mathcal{C}'$

$$T = \text{Min}\left(1, \frac{L - 2M' + 1}{L - 2M + 1} e^{-\sum_j \lambda_j(\mathcal{I}_j' - \mathcal{I}_j)}\right). \qquad (18)$$

Here λ_j are the Lagrange multipliers, and $\mathcal{I}_j$ is the expectation value of the conserved charge on the eigenstate identified by the Bethe-Takahashi quantum numbers $\mathcal{C}$.

In (18) the factor $L - 2M + 1$ corresponds to the S_z degeneracy in the sector with M particles. Crucially, the Metropolis acceptance probability (18) relies on the fact that the conserved charges $\mathcal{I}_j$ are $SU(2)$ scalars.

The procedure outlined above defines a Markov chain. After a thermalization time the configurations generated are distributed according to the GGE probability (1).

Notice that step 1 and 2 take into account the density of the states of the XXX chain, while step 5 generates the correct GGE probability (1).

IV. EXTRACTING THE RAPIDITY DENSITIES

The rapidity densities ρ_n^p of the ensemble representative state can be measured in Monte Carlo from the histograms of the roots generated in the Monte Carlo history.

This is illustrated in Fig. 2 for several ensembles. In the Figure panels (a)-(c) plot the first three root densities $\rho_n(x)$ for $n = 1, 2, 3$ as a function of x for the representative state of the infinite-temperature Gibbs ensemble. We restrict ourselves to the interval $-6 \leq x \leq 6$. In each panel the different histograms correspond to different chain sizes $18 \leq L \leq 30$. The histograms are obtained from $4 \cdot 10^5$ Monte Carlo steps. The width of the histogram bins is given as $2/L$. In all the panels the full lines are the analytic results obtained from the Thermodynamic Bethe Ansatz (TBA) (cf. (21)). Remarkably, although finite-size effects are present, the Monte Carlo data are in good agreement with the TBA results. This is especially true for ρ_1, whereas finite-size corrections become progressively worse upon considering larger $n > 1$ (see panels (b)(c)). Clearly, these corrections are vanishing upon increasing the system size (see for instance the arrow in panel (b)). Moreover, the finite size effects become larger upon increasing the rapidity x. This is expected as larger rapidity correspond to larger quasi-momenta, which are more sensitive to the lattice effects. Finally, finite-size effects increase with n. This is somewhat expected since larger n correspond to more extended many-spin bound states.

Finite-temperature ensemble can be also considered. This is illustrated in panel (g) discussing the Gibbs ensemble at inverse temperature $\beta = 1/2$ and $\beta = 1$ (different histograms in the panel). We focus on $\rho_1(x)$ The data for infinite temperature are reported for comparison. All the histograms are obtained for $L = 30$. The full lines are now the analytic results obtained by solving the TBA equations and perfectly agree with the Monte Carlo data. Notice that upon lowering the temperature the height of the zero rapidity peak increases. This reflects that at $T = 0$ the ground state of the antiferromagnetic Heisenberg chain are packed around $x = 0$, and the contribution of nonzero rapidity is vanishing exponentially.

Finally, in panels (d)(f) we present the rapidity densities $\rho_n(x)$ for the GGE ensemble. Specifically, here we focus on the GGE obtained including the two charges $\mathcal{I}_2$ and $\mathcal{I}_4$. We fix the associated Lagrange multipliers to $\lambda_2 = 0$ and $\lambda_4 = 1$. Similar to the Gibbs ensemble, panels (a)(c) suggest that for $L = 30$ the finite size effects are negligible, at least in the interval $-2 \leq x \leq 2$.
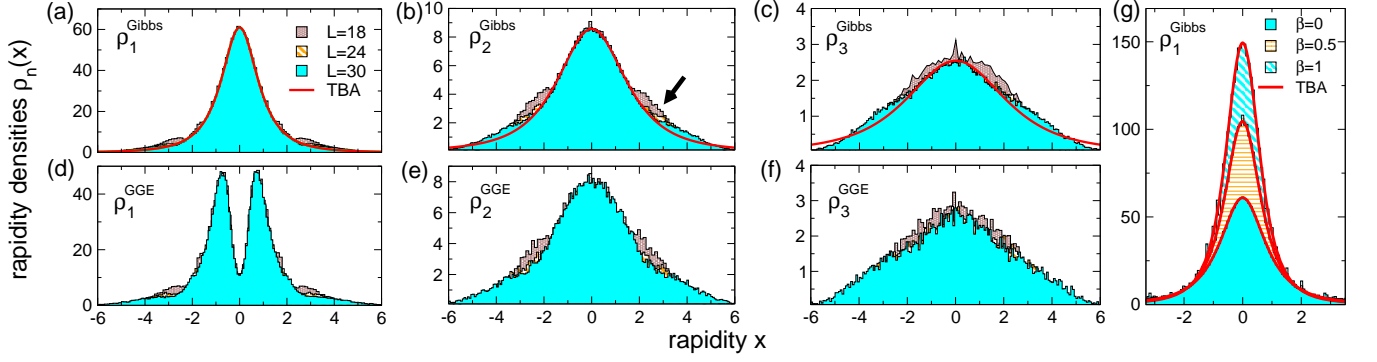
FIG. 1. The rapidity densities $\rho_n(x)$ (for $n = 1, 2, 3$) for the infinite temperature Gibbs (panels (a)-(c)) and the GGE equilibrium states (panels (d)-(f)): Numerical results for the Heisenberg spin chain obtained using the Hilbert space Monte Carlo sampling. Here the GGE is constructed including only $\mathcal{I}_2$ and $\mathcal{I}_4$ with fixed Lagrange multipliers $\lambda_2 = 0$ and $\lambda_4 = 1$. In all the panels the data are the histograms of the n-strings rapidities sampled in the Monte Carlo. The width of the histogram bins is $\Delta x = 2/L$. In each panel different histograms correspond to different chain sizes L. All the histograms are divided by 10^3 for convenience. In (b) the arrow is to highlight the finite-size effects. In panels (a)-(c) the lines are the Thermodynamic Bethe Ansatz (TBA) results. (g) Finite-temperature effects: Monte Carlo data for ρ_1^{Gibbs} for different values of the inverse temperature β.
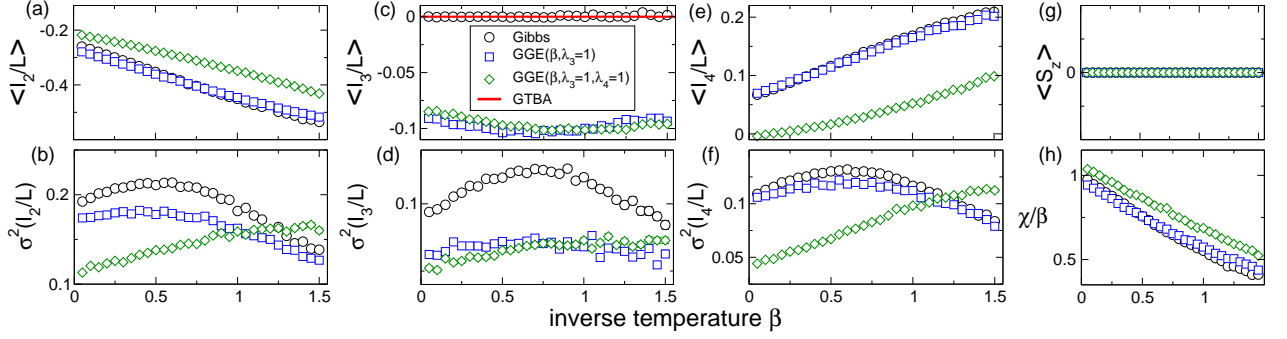

FIG. 2. The Generalized Gibbs Ensemble (GGE) for the Heisenberg spin chain with $L = 16$ sites: numerical results obtained using the Hilbert space Monte Carlo sampling. Only the first three conserved charges $\mathcal{I}_n$ ($n = 1, 2, 3$), with associated Lagrange multipliers λ_n, are included in the GGE. Here $\mathcal{I}_2$ is the Hamiltonian and $\lambda_2 \equiv \beta$ the inverse temperature. In all the panels different symbols correspond to different values of λ_3, λ_4. The circles correspond to the Gibbs ensemble, i.e., $\lambda_3 = \lambda_4 = 0$. (a) The GGE average $\langle \mathcal{I}_2/L \rangle$ plotted as a function of β. (b) Variance of the GGE fluctuations $\sigma^2(\mathcal{I}_2/L) \equiv \langle (\mathcal{I}_2/L)^2 \rangle - \langle \mathcal{I}_2/L \rangle^2$ as a function of β. (c)(d) and (e)(f): Same as in (a)(b) for $\mathcal{I}_3$ and $\mathcal{I}_4$, respectively. In all panels the dash-dotted lines are the analytical results obtained using the Generalized Thermodynamic Bethe Ansatz (GTBA). (g) The GGE expectation value of the total magnetization $\langle S_z \rangle$. Notice that $\langle S_z \rangle = 0$ due to the $SU(2)$ invariance of the conserved charges. (h) χ/β plotted versus β, with χ being the magnetic susceptibility per site.

V. LOCAL OBSERVABLES

We now turn to discuss the behavior of some *local* observables. This is discussed in Fig. 2. Here we focus on GGE expectation values of local obervables. Here the GGE is constructed including the conserved charges $\mathcal{I}_j$ with $j = 2, 3, 4$. In the Figure we consider several values of the associated Lagrange multipliers, namely $\lambda_3 = 0$ and $\lambda_4 = 0$ (Gibbs ensemble, circles in the Figure), $\lambda_3 = 1$ and $\lambda_4 = 0$ (squares in the Figure), and $\lambda_3 = \lambda_4 = 1$ (rhombi). All the data are obtained using the Monte Carlo sampling approach for a chain with $L = 16$ sites. The expectation values are the Monte Carlo averages of the local observables over the eigenstates sampled by the Monte Carlo. All the expectation values are plotted versus the inverse temperature $\lambda = \beta$. Panel (a) focuses on the GGE expectation value of energy density

$\langle \mathcal{I}_2 \rangle/L$. The variance of the associated ensemble fluctuations $\sigma^2(\mathcal{I}_2/L) \equiv \langle (\mathcal{I}_2/L)^2 \rangle - \langle \mathcal{I}_2/L \rangle^2$ are shown in panel (b). The latter are related to the specific heat of the chain.

As expected, different GGEs (different symbols in the Figure) implies different behaviors of $\langle \mathcal{I}_2/L \rangle$ as a function of β. The continuous lines are the analytic results obtained by solving the GTBA equations. Remarkably, the latter fully match the Monte Carlo data, i.e., finite-size effects are negligible already at $L = 16$.

How do I reconcile this with Fig. 1 where finite size effects are visible even for $L = 30$. Is that true that shorter correlations are less sensitive to higher momenta?

This remains true if one considers the GGE expectation values of operators with larger supports.

For instance, this is confirmed for the energy current $\mathcal{I}_3 \equiv \sum_{\alpha\beta\gamma} \epsilon_{\alpha\beta\gamma} \sigma_i^\beta \sigma_{i+1}^\gamma \sigma_{i+2}^\alpha$ in panels (c)(d). Notice that for the
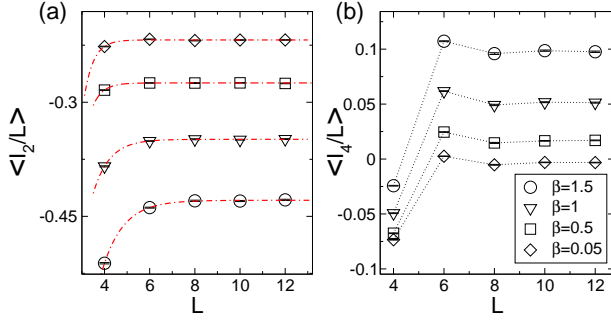
FIG. 3. Finite-size scaling of the GGE averages in the Heisenberg chain: Numerical results obtained from the Hilbert space Monte Carlo sampling. Here the GGE is constructed including $\mathcal{I}_2, \mathcal{I}_3, \mathcal{I}_4$, with Lagrange multipliers $\lambda_2 = \beta, \lambda_3 = \lambda_4 = 1$. (a) $\langle \mathcal{I}_2/L \rangle$ plotted versus the chain size L for several values of β. The dash-dotted lines are exponential fits. (b) Same as in (a) for $\mathcal{I}_4$.

Gibbs ensemble one has $\langle \mathcal{I}_3 \rangle = 0$, due to the parity invariance. Similar behavior is observed for $\mathcal{I}_4$ in panels (e)(f).

Finally, in panels (g)(h) we focus on the total magnetization $\langle S_z \rangle$ and the spin susceptibility χ.

VI. THE STRING ROOT DENSITIES AT INFINITE TEMPERATURE

For infinite temperature the densities ρ_n are given as

$$\rho_n(x) = \frac{2}{\pi} \frac{1}{(n^2 + x^2)(x^2 + (2 + n)^2)} \tag{19}$$

Notice that

$$\int_{-\infty}^{+\infty} \rho_n(x) dx = \frac{1}{n(n+1)(n+2)} \tag{20}$$

Icluding the first order correction to the infinite temperature result one obtains

$$\rho_n(x) = \frac{2}{\pi} \frac{1}{(n^2 + x^2)(x^2 + (2 + n)^2)}$$
$$- \frac{8}{\pi} \frac{n(n+2)}{(n^2 + x^2)^2(x^2 + (2 + n)^2)^2} J\beta + \mathcal{O}(J^2\beta^2) \tag{21}$$